Protein Ion-Exchange Adsorption Kinetics

J. A. Wesselingh
Chemical Engineering Dept., University of Groningen, Nijenborgh 4, 9747 AG Groningen, The Netherlands

J. C. Bosma
Dept. of Industrial Pharmacy, University of Groningen, 9713 AV Groningen, The Netherlands

The kinetics of the adsorption of the protein BSA on the ion exchanger Q-Sepharose FF were measured for several values of the pH and ionic strength, using several techniques. The measurements were best described with a model incorporating both surface and pore diffusion and with the chemical potential gradient as the driving force for diffusion. The surface-diffusion coefficients from this model show an inverse exponential dependency on the binding strength. This dependency can be explained by an activated jump mechanism. The pore-diffusion coefficient is much lower than that in free solution, which is probably caused by a combination of steric and electric exclusion.

Introduction

Ion-exchange chromatography is widely used for the purification of proteins. In this process the adsorption kinetics are important; they control the sharpness of peaks and breakthrough curves.

Recently various articles have been published on this subject. Habbaba and Ülgen (1997) present relatively simple models. Yoshida et al. (1994) use more sophisticated models and show that both pore diffusion and surface diffusion play a role. Karst Lewus and Carta (1999) consider the kinetics of competitive adsorption of two proteins.

This article presents measurements and models of the adsorption kinetics of a protein on an ion exchanger at varying pH and ionic strength. The goal is to demonstrate which physical processes are important and how they depend on the pH and the ionic strength.

Theory

Adsorption kinetics models

When proteins adsorb, two processes can limit the adsorption rate: slow diffusion and slow adsorption. The kinetics of the actual adsorption can be slow if a protein has to rearrange its three-dimensional structure in order to adsorb. For our model system we have assumed that the adsorption is instantaneous. There are two reasons for this:

- The adsorption equilibrium depends mainly on electrical forces (Bosma and Wesselingh, 1998); these are instantaneous.
- Unfolding of proteins may occur on hydrophobic surfaces because the groups inside a protein are attracted by the surface. The surface of our ion exchanger is strongly hydrophilic, however, and proteins should not unfold.

There are two steps in the diffusion up to the pore wall:

- Diffusion from the pore bulk to the pore wall. We neglect this step, as the diffusion distance is very small. This implies that we assume local adsorption equilibrium in the pores.
- Diffusion toward or away from the center of the particle.

Below we present two models for the finite bath adsorption experiments: the homogeneous model and the two-phase diffusion (TPD) model. In both models only diffusion of the protein is considered. It is assumed that small ions diffuse rapidly and have no effect on the transport of the proteins. Both models consider the protein concentration profile inside the particle.

The mass balance outside the particle gives

$$\frac{1-\epsilon_{\text{particle}}}{\epsilon_{\text{particle}}}\frac{dc}{dt} = -\frac{d\bar{q}}{dt} = \frac{D}{\delta_l}a(c_{p,R}-c). \qquad (1)$$

Here c is the protein concentration in the bulk liquid, q is the protein concentration in the particle, $\bar{q}$ is the average of q, $\epsilon_{\text{particle}}$ is the particle holdup, a is the particle surface per particle volume, $c_{p,R}$ is the concentration in the pores at the surface of the particle, D is the diffusion coefficient in liquid, and δ_l is the liquid-film thickness. According to Calderbank and Moo-Young (1961), there are two mass-transfer regimes: one in which mass transfer is controlled by sedimentation of the particles, and one in which turbulence causes the mass transfer to be faster. We performed our experiments in the first regime, and the thickness of the mass-transfer film is

Correspondence concerning this article should be addressed to J. C. Bosma.

given by

$$\delta_l = \frac{d_p}{0.31}\left(\frac{\mu}{\Delta\rho g D^2}\right)^{1/3} \tag{2}$$

where μ is the viscosity, $\Delta\rho$ is the density difference, and g is the gravitational acceleration.

The mass balance inside the particle gives

$$\frac{dq}{dt} = \frac{1}{r^2}\frac{d}{dr}\left[r^2 D_{\text{eff}}\frac{dq}{dr}\right]. \tag{3}$$

In the homogeneous model, we assume that the particle is homogeneous and that the effective-diffusion coefficient is independent of the concentration. In the two-phase diffusion (TPD) model we assume that two transport processes occur in parallel: diffusion of proteins in the pore bulk and diffusion of adsorbed proteins on the pore walls. The total adsorbed concentration, q, is the sum of the concentration in the pore bulk, c_p, and the adsorbed concentration at the surface, q_s

$$q = \epsilon_p c_p + q_s. \tag{4}$$

Here ϵ_p is the pore holdup. The driving force for diffusion is the chemical potential gradient. We assume that the proteins in the pore bulk behave ideally, so their activity coefficient is independent of concentration. Therefore diffusion in the pore bulk can be described by Fick's law

$$\phi_p = D_p\frac{dc_p}{dr}. \tag{5}$$

At the pore walls the driving force is the same since we assume local adsorption equilibrium. The expression for the diffusive flux at the walls becomes

$$\phi_s = \frac{q_s}{c_p}D_s\frac{dc_p}{dr}. \tag{6}$$

This is better than assuming that Fick's law can be used at the surface, as is shown for the surface diffusion of alkanes by Kapteijn et al. (1995). Our approach is a simplification of the Maxwell-Stefan approach (see Wesselingh and Krishna, 2000). The total flux is given by

$$\phi = \epsilon_p\phi_p + \phi_s = D_{\text{eff}}\frac{dq}{dr}. \tag{7}$$

An expression for the effective diffusion coefficient, D_{eff}, can be derived from Eqs. 4 to 7

$$D_{\text{eff}} = \frac{\epsilon_p D_p + \frac{q_s}{c_p}D_s}{\epsilon_p + \frac{dq_s}{dc_p}} \tag{8}$$

A description of the equilibrium is needed for both models: in the TPD model for the local equilibrium in the pores, and in the homogeneous model for the surface of the particle. In a previous study of the adsorption equilibrium we found that the steric mass action (SMA) model describes equilibrium well (Bosma and Wesselingh, 1998). This model assumes that adsorption is an exchange reaction of a protein with a number of small ions. The equilibrium depends on ionic strength and pH; however, the effect of these two can be combined in a single parameter. This is the concentration in the liquid at which the adsorption has one half of its maximum value—the "half-concentration." Figure 1 shows examples of adsorption isotherms for different half-concentrations. Figure 2 shows the dependence of the half-concentration on the pH and the ionic strength for our experimental system.

We have tested many other models for the rate of adsorption, but will only mention them in the discussion section.

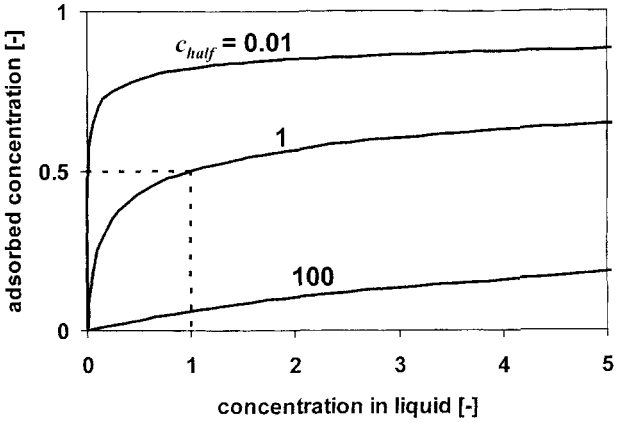

Figure 1. Isotherms of BSA binding on Q-Sepharose FF at various half-concentrations; the dotted lines illustrate the physical meaning of the half-concentration for the middle isotherm.

Experimental Studies

Materials

All experiments were performed with bovine serum albumin (BSA) from Boehringer Mannheim and Q-Sepharose FF

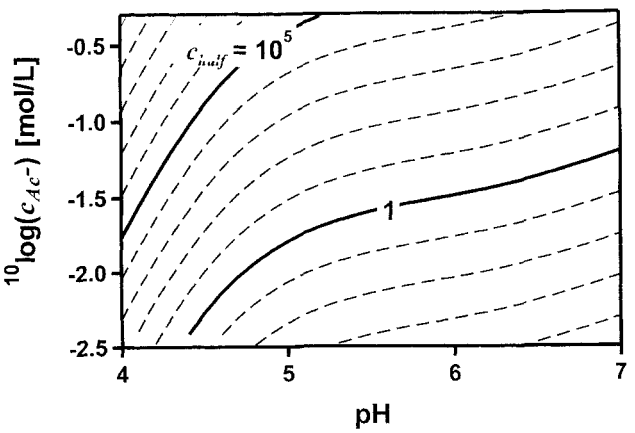

Figure 2. Isoadsorption lines giving the effect of pH and ionic strength on the half-concentration of BSA binding on Q-Sepharose FF in an acetate buffer.

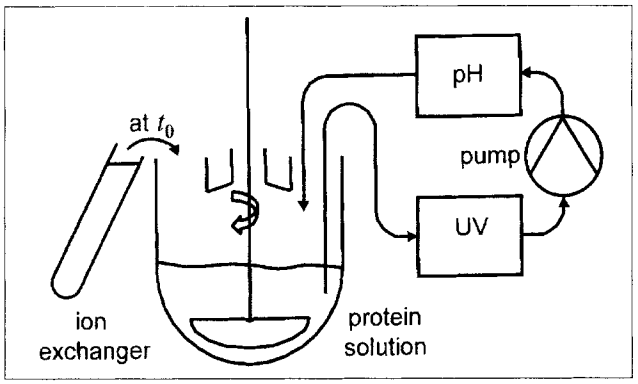

Figure 3. Experimental setup for the batch-adsorption experiments.

from Pharmacia Upjohn.

Batch-adsorption experiments

The experimental setup is shown in Figure 3. Batch-adsorption experiments of BSA adsorbing on Q-Sepharose FF in acetate buffers were performed in 250-mL flasks, stirred at 200 rpm. By pumping the solution through a UV adsorption meter ($\lambda = 280$ nm) and a pH meter these parameters were continuously monitored. For an experiment a flask was filled with 140 mL of a protein solution in the appropriate acetate/acetic acid buffer. After that a known amount of ion exchanger, suspended in water, was added. This was 5 to 7 mL (sedimented bed volume) of ion exchanger in an amount that totaled 10 mL. After adding the ion exchanger, the UV adsorption and the pH were monitored for 1 to 5 h. Some adsorption–desorption experiments were also performed, in which after a certain adsorption time a salt solution was added to induce desorption.

The conditions of the experiments were: pH between 4.5 and 6.3, ionic strength between 1 and 100 mM, and BSA concentration at the start between 2 and 20 g/L. Some experiments were performed at lower and higher stirrer speeds: at speeds above 200 rpm, adsorption was not accelerated. In a few experiments a certain amount of water (instead of water with ion exchanger) was added to measure how fast a concentration change was detected by the UV meter. The measured concentration approached the real one exponentially with a half time of 14 s. In comparing the measured and calculated results the following transformation was applied to the *calculated* results

$$c_{UV}(t) = \frac{\int_{-\infty}^{t} c(\tau)\exp[0.048(\tau - t)]\,d\tau}{\int_{-\infty}^{t} \exp[0.048(\tau - t)]\,d\tau}. \qquad (9)$$

Confocal microscopy experiments

A few experiments were performed with confocal microscopy. This technique measures concentration profiles inside a particle. A confocal microscope can focus on a thin slice of a transparent object. In this slice it measures the light intensity at a certain wavelength. In our experiments we used BSA that was dyed with Cy-2 fluorescent dye (obtained from Pharmacia Upjohn). A laser beam, at 488 nm, was used to excite the dye, and the emitted light intensity at 515 nm was measured. In an experiment we first made solutions of the dyed protein and dilute suspensions of the ion exchanger in the appropriate buffers. Then we put a small amount of the ion-exchanger suspension on the object glass, removed most of the excess liquid by adsorbing it with a paper tissue, added the protein solution, and put a cover glass over it. Finally, we put the final assembly under the microscope and followed the concentration profile. The microscope was an ODYSSEY real-time laser confocal microscope from Noran Instruments. Its software can save the measured intensities with a very high frequency; however, it can only save the average concentrations in eight regions. We chose to monitor the concentrations in a row of squares ranging from the center of a particle to the edge or a little further out. The results is the development of a light-intensity profile in the particle. To obtain the concentration profile we assumed that the light intensity was linearly dependent on the concentration. Because we could not calibrate the system, the results are qualitative.

Solution of the models

The two models were solved on the computer. For the TPD model the effective diffusion coefficient as a function of the concentration in the particle, q, was calculated using Eq. 8. Both models were solved by calculating the concentration at 50 discrete locations inside the particle.

In our calculations we used:

- A protein adsorption capacity of 150 g/L, based on the particle volume;
- A pore holdup in the particle, ϵ_p, of 0.52, which equals the partition coefficient of the protein at high ionic strength;
- A particle diameter of 95 μm;
- A liquid side film thickness of 14 μm (calculated with Eq. 2).

Results

The parameters in the batch adsorption experiments are summarized in Table 1. Two examples are given in Figures 4 and 5. Figure 6 shows the surface-diffusion coefficients as a function of the binding strength for the two models. The correlation coefficients that were calculated for each model from the data in Figure 6 and for one other model are given in Table 2. In the TPD model two diffusion coefficients have to be fitted: we assumed that the pore-diffusion coefficient is constant during all the experiments and fitted the surface-diffusion coefficient. The correlation coefficients that were calculated for various pore diffusion coefficients are given in Figure 7. A value of 9×10^{-13} m^2/s for the pore-diffusion coefficient gave the best correlation, but this value is not critical.

Two examples of batch adsorption–desorption experiments are given in Figures 8 and 9. The desorption part of the lines of the homogeneous model were calculated by fitting the effective-diffusion coefficient. In the TPD model we used the surface-diffusion coefficient obtained by the equation in Table 2 with a pore-diffusion coefficient of 2×10^{-11} m^2/s during desorption. For lower pore-diffusion coefficients the agreement with experiment is much poorer. With the fitted pore-diffusion coefficient, the agreement is still not good, but

Table 1. Summary of the Batch Adsorption Experiments

Exp. No.	pH	c_{Ac} [mM]	c_0 [g/L]	c_{eq} [g/L]	c_{ball} [g/L]	$10^{13}\ D_{hom}$ [m^2/s]	$10^{13}\ D_{s,TPD}$ [m^2/s]	ϕ_s/ϕ
1	5.53	100	9.8	9.16	1080	14.9	10.5	0.92
2	5.60	100	9.8	9.24	1284	15.0	11.0	0.91
3	5.50	20	9.9	7.82	1.24	4.59	0.970	0.78
4	5.42	5	9.9	6.38	5.18×10^{-1}	2.77	0.279	0.64
5	4.47	20	10.3	9.02	319	16.0	8.82	0.94
6	4.96	20	10.4	7.98	9.42	5.90	1.73	0.87
7	5.51	20	9.9	6.95	0.403	2.59	0.458	0.70
8	5.35	10	10.0	6.30	0.0343	1.83	0.224	0.61
9	5.49	50	10.0	7.92	23.5	7.11	2.49	0.90
10	5.57	20	2.0	0.09	0.168	1.45	0.350	0.97
11	5.54	20	5.0	2.60	0.272	2.82	0.567	0.89
12	5.50	20	10.0	7.93	0.480	3.74	0.682	0.76
13	5.53	20	20.0	14.9	0.0154	8.79	1.02	0.83
14	4.92	5	2.0	0.01	0.0429	0.717	0.147	0.99
15	4.88	5	5.0	1.11	0.0353	1.07	0.166	0.83
16	4.92	5	10.0	6.31	0.0420	1.76	0.224	0.61
17	4.89	5	15.0	11.5	0.0559	3.57	0.443	0.64
18	4.78	5	10.0	6.75	0.0654	1.59	0.209	0.61
19	4.81	10	10.0	7.33	0.773	3.57	0.709	0.81
20	4.80	50	10.2	9.29	658	8.74	5.42	0.89
21	5.46	5	2.0	0.02	0.00226	0.722	0.099	0.94
22	5.51	10	2.0	0.09	0.0189	0.976	0.174	0.95
23	5.51	20	2.0	0.19	0.302	2.16	0.561	0.98
24	5.49	50	2.0	1.14	32.3	7.05	3.53	0.98
25	5.52	100	2.0	1.63	552	6.98	5.79	0.96
26	6.00	100	10.0	9.06	222	8.30	4.22	0.89
27	5.98	100	2.0	1.44	197	10.4	7.16	0.98
28	6.00	100	5.0	4.15	199	7.92	4.65	0.94
29	6.00	100	15.0	14.2	424	5.95	2.97	0.74
30	6.01	50	2.0	0.63	4.89	4.37	1.64	0.98
31	4.27	1	9.9	6.45	0.0434	1.31	0.156	0.53
32	5.06	1	10.0	5.76	7.15×10^{-5}	0.640	0.0286	0.19
33	6.00	1	10.0	6.02	7.47×10^{-7}	0.373	0.00497	0.033
34	6.25	20	9.9	7.14	0.0633	1.81	0.225	0.53
35	5.50	2	10.0	6.28	1.01×10^{-4}	0.823	0.0397	0.20
36	5.90	1	10.0	5.50	6.84×10^{-7}	0.298	0.00395	0.029
37	5.95	1	10.0	6.31	1.23×10^{-7}	0.283	0.00429	0.035
38	5.50	1	10.0	6.19	2.06×10^{-6}	0.404	0.00856	0.063
39	5.50	5	10.0	7.45	5.58×10^{-4}	0.599	0.0326	0.18
40	5.45	10	10.0	7.03	0.0105	1.27	0.129	0.47
41	6.03	20	10.0	6.74	0.0176	1.30	0.140	0.51
42	4.60	1	10.0	5.99	1.74×10^{-3}	1.39	0.119	0.51

the curvatures of the concentration histories just before the maximum of the measured and calculated curves show the best agreement. There is still great uncertainty in this pore-diffusion coefficient. Figures 10 through 12 give both the calculated concentration profiles in a particle at various binding strengths and the concentration profiles that were measured with confocal microscopy under the same conditions.

Discussion

This discussion will be extensive. First we compare the two models and their results in four ways. The TPD model will turn out to be the best model, and we discuss the mechanisms of the pore and the surface diffusion and their relative importance. Finally we discuss some deficiencies in the TPD model.

Comparing the models

The models can be evaluated in four ways.

First the predicted histories of the protein concentration in the stirred tank can be compared with the measurements; this is done in Figures 4 and 5. Both models give results that are similar to the measurements. The difference between the models and the measurements can be explained by the effect of the particle-size distribution. We found that when the particle-size distribution is first included in a model, the adsorption is faster (due to the higher particle surface), while at the end it is slower (due to the large particles). The concentration histories do not allow us to draw any conclusions.

The second way to compare the models is by evaluating the correlation between the calculated diffusion coefficients and the binding strength. We found that the binding strength can be used to represent the effect of the pH and the ionic strength. The correlations are shown in Figure 6 and Table 2.

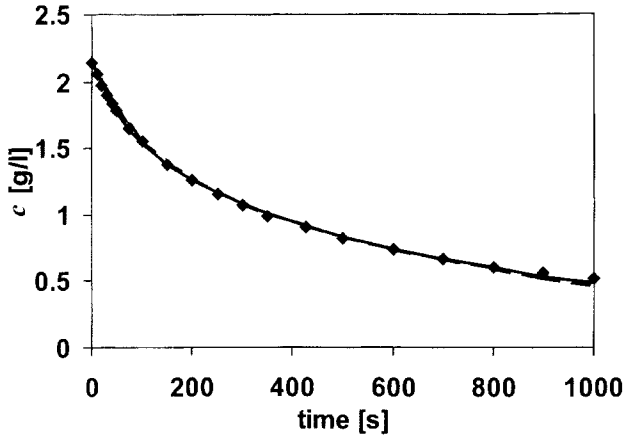

Figure 4. Example of an adsorption curve at a starting concentration of 2 g/L (exp. 10).

– – – –TPD model; —— homogeneous model.

The homogeneous model gives a correlation that is quite good. If we introduce the dependence of the diffusion coefficient on the starting concentration, we find an even better correlation (see Table 2). The TPD model gives the best correlation, as it shows a surface-diffusion coefficient that changes sharply with the half-concentration.

The third way to compare the models is to compare the predicted concentration histories of the adsorption–desorption experiments with the measurements. This is done in Figures 8 and 9. These figures show that the addition of a salt solution causes rapid desorption followed by little readsorption. In our calculations the homogeneous model never predicts readsorption. The TPD model can predict readsorption, but the predicted maximum in the adsorption curve is much lower than the measured one.

The fourth way to compare the models is with the results of the confocal microscopy experiments. Figures 10 through 12 show some calculated concentration profiles inside the particle during adsorption. The TPD model predicts that:

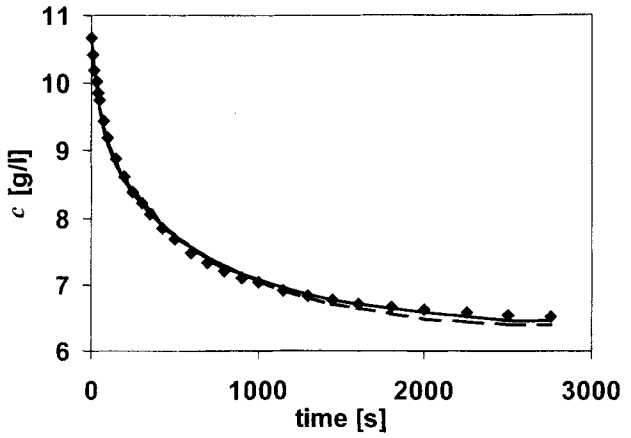

Figure 5. An example of an adsorption curve at a starting concentration of 10 g/L (exp. 4).

– – – – TPD model; —— homogeneous model.

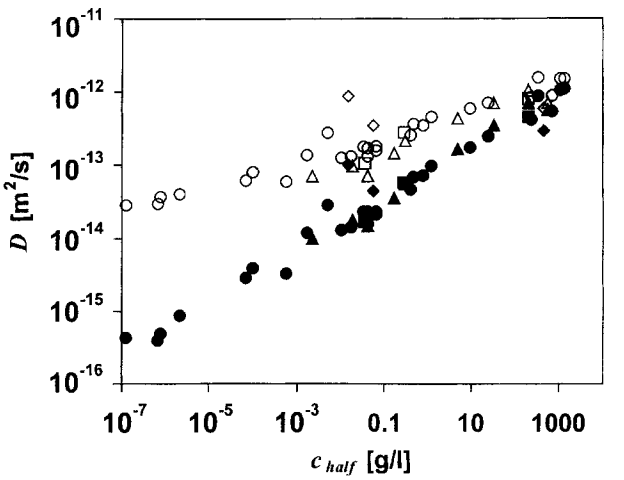

Figure 6. Calculated diffusion coefficients according to the models vs. the half-concentration.

For the TPD model these are surface-diffusion coefficients, for the homogeneous model effective-diffusion coefficients. Symbols: open-homogeneous model; closed: TPD model; approximate average protein concentration: △ –2 g/L, □ –5 g/L, ○ –10 g/L, ◇ –15 or 20 g/L.

- The concentration profiles have an inflexion point, where the concentration gradient has a maximum.
- The concentration gradient at the inflexion point increases sharply with increasing binding strength.

The homogeneous model predicts concentration profiles that are practically independent of the binding strength. In Figures 10 through 12 it can be seen that the qualitative effects that the TPD model predicts are also measured. This means that the TPD model is better. However, the sharpness of the measured concentration profiles is less than that of the calculated profiles. There are explanations for this and they are discussed in the subsection on "Differences Between the TPD Model and the Measurements." Overall the homogeneous model is not bad either. However, it predicts a less steep profile then the measured one, without an inflexion point, and we cannot explain why a measured profile can be steeper than a theoretical one.

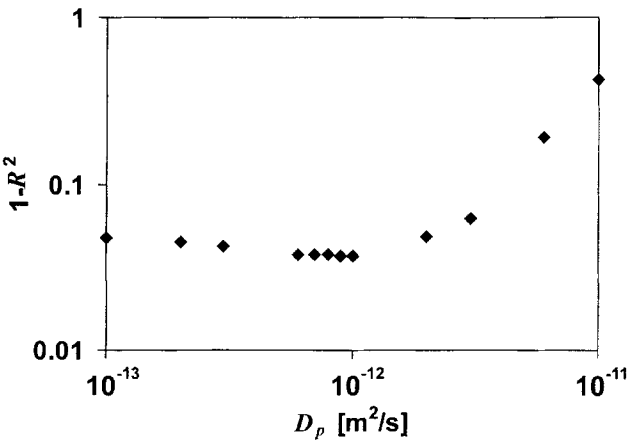

Figure 7. Correlation between the half-concentration and the surface-diffusion coefficient at various assumed pore diffusion coefficients in the TPD model.

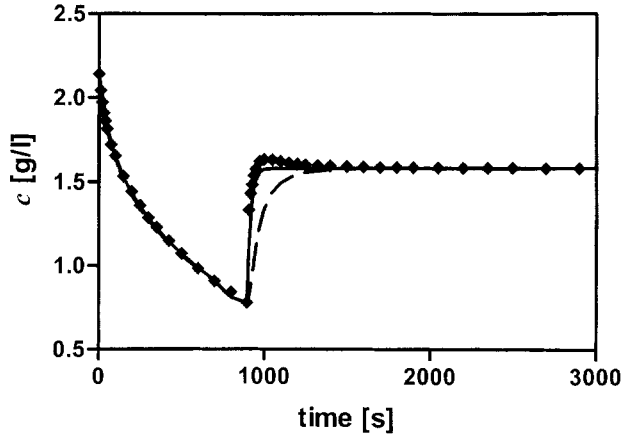

Figure 8. Example of an adsorption—desorption curve at a starting concentration of 2 g/L.

– – – – TPD model; —— homogeneous model. The pH was 5.3 and the ionic strength changed from 5 to 100 mM.

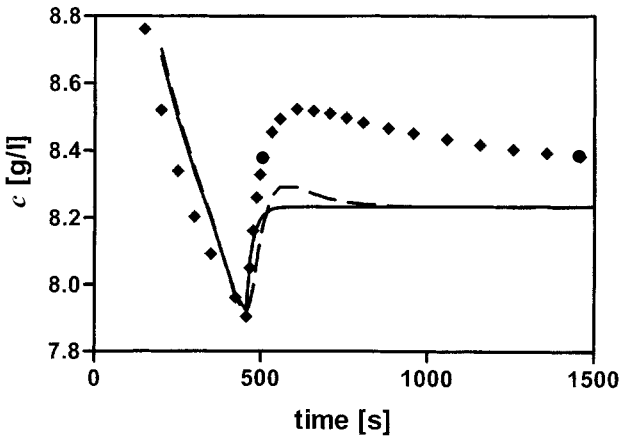

Figure 9. Example of an adsorption—desorption curve at a starting concentration of 10 g/L.

– – – – TPD model; —— homogeneous model. The pH was 5.3 and the ionic strength changed from 20 to 50 mM.

Overall we conclude that the TPD model is the best model. The main reason is that it uses the chemical potential gradient as the driving force. Two reasons for this conclusion are:

- The diffusion coefficient in the homogeneous model depends on the concentration (see Table 2). In the TPD model the pore- and surface-diffusion coefficients are independent of concentration. Apparently the effect of the concentration on the effective-diffusion coefficient is satisfactorily described by Eq. 8.
- The measured inflexion point in the concentration profile inside a particle cannot be modeled using the concentration gradient as the driving force. We found that the inflexion point in the TPD model is not caused by diffusion in the two phases, but by the use of the chemical potential gradient as the driving force.

Simpler model

We just concluded that the TPD model is the best; however, in some cases it is not the most useful. For example, when a column process is modeled numerically the calculation of the concentration profile inside all particles may be too time-consuming. A simpler model that only considers one (possibly lumped) mass-transfer resistance between the liquid and the particle phase may be better.

The best model that we found that does not calculate the concentration profile inside the particle is a linear-driving-force model with the chemical potential difference as the driving force for diffusion. As in Eq. 6, a factor q/c will appear in the flux equation. The logarithmic mean of the factor in both phases was used for this factor.

For the total mass transfer (neglecting the liquid-side mass-transfer resistance) we used:

$$\frac{1-\epsilon_{\text{particle}}}{\epsilon_{\text{particle}}}\frac{dc}{dt} = -\frac{dq}{dt} = \frac{10D_{\text{eff}}}{d_p}a[c(q)-c]\sqrt{\frac{q}{c(q)}\frac{q(c)}{c}} \tag{10}$$

Here $c(q)$ is the unadsorbed concentration that would be at equilibrium with the adsorbed concentration q and $q(c)$ is the adsorbed concentration that would be in equilibrium with the unadsorbed concentration c. For high initial concentrations the prediction of the initial adsorption rate is too high

Table 2. Fitted Straight Lines in Figure 6 According to $D = D_0 \cdot c_{\text{half}}^p$

Model	D_0 [m²/s]	P	R^2
Homogeneous	3.36×10^{-13}	0.171	0.85
Homogeneous	$2.18\times10^{-13}\times1.051^{c_0}$	$0.248-0.0072\ c_0$	0.928
TPD	7.81×10^{-14}	0.346	0.963
LDF	2.14×10^{-14}	0.556	0.981

The D's in the TPD model are surface-diffusion coefficients, while those for the other models are effective-diffusion coefficients.

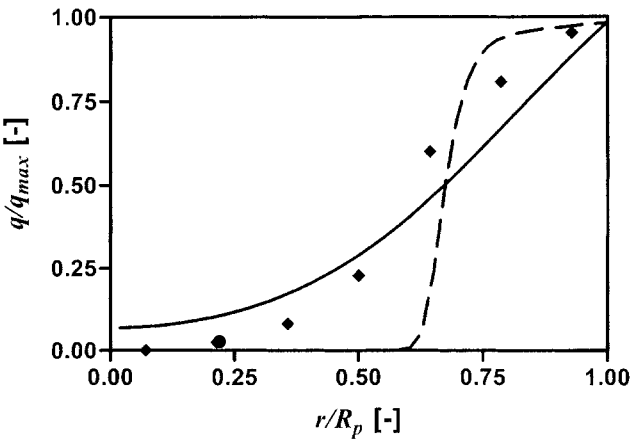

Figure 10. Concentration profile in the particle during adsorption at $c_{\text{half}} = 6.3\times10^{-6}$ (pH 5.9 and $c_{Ac^-} = 1$ mM) after 3,000 s.

– – – – TPD model; —— homogeneous model: ♦—measurements.

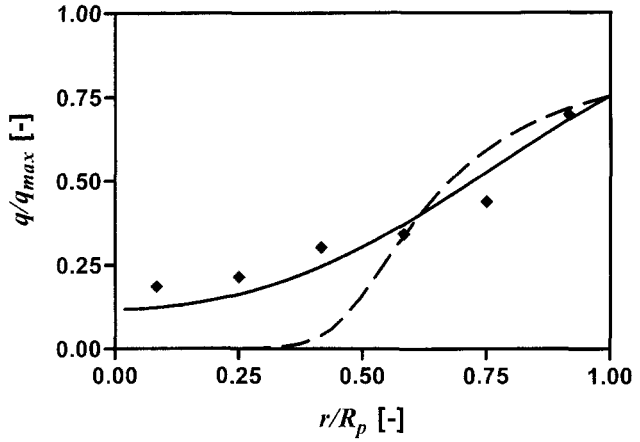

Figure 11. Concentration profile in the particle during adsorption at c_{half} = 0.13 (pH 4.8 and c_{Ac^-} = 5 mM) after 679 s.

– – – – TPD model; —— homogeneous model; ♦ —measurements.

and the final adsorption rate too low. It is the other way around for low concentrations. The model gives a good correlation between the the binding strength and the diffusion coefficient (see Table 2, LDF model).

The surface-diffusion mechanism

In Figure 6 it can be seen that there is a close relationship between the half-concentration and the surface-diffusion coefficient. This relationship can be explained by an activated jump mechanism. To jump from one adsorption site to the next, the protein has to overcome an activation barrier with free energy μ_a. An adsorption site is a site where the binding sites (ionic groups) of the protein and the ion exchanger fit together. It is probable that these sites overlap. The activated jump mechanism gives rise to an Arrhenius type of dependence:

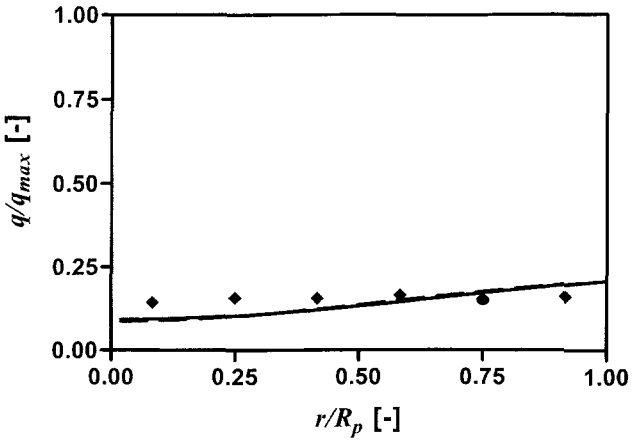

Figure 12. Concentration profiles in the particle during adsorption at c_{half} = 720 (pH 4.5 and c_{Ac^-} = 20 mM) after 250 s.

– – – – TPD model; —— homogeneous model; ♦ measurements.

$$D_s = D_{s,0} e^{-\mu_a/RT}. \tag{11}$$

It is reasonable to assume that the activation free energy will be proportional to the free energy change of adsorption. This free energy change contains both the electrical adsorption energy and an entropic contribution of the salt concentration in the bulk liquid. For our materials we found (Bosma and Wesselingh, 1998) that it depends on the half-concentration via an Arrhenius-type equation

$$c_{half} = c_{half,0} e^{-\Delta\mu_{ads}/RT}. \tag{12}$$

When these two equations are combined it follows that there should be a linear relationship between the logarithm of the surface-diffusion coefficient and the logarithm of the half-concentration. In Figure 6 we see that the activation free energy is 34% of the free energy of adsorption (the slope is 0.34).

The value of the unimpeded diffusion coefficient, $D_{s,0}$, should be approximately equal to the value given by the Einstein equation: $u\lambda/4$, in which λ is the jump length and u is the thermal velocity. The thermal velocity is approximately

$$u \approx \sqrt{\frac{3RT}{M}}. \tag{13}$$

Using the data in Figure 6 and our previous results, we get a jump length of only 0.004 nm. Although there are many more ion-exchange groups than necessary for binding, it is unrealistic to assume that the adsorption sites are so close together. We think that the adsorption sites are about one hundred times further apart. The discrepancy is probably caused by viscous friction between the protein and water. It is also possible that jumps fail due to the protein being incorrectly oriented or a jump in the wrong direction.

Electrical-exclusion effect

Electrical exclusion affects the unadsorbed protein concentration in the pores. It can greatly decrease the diffusive flux of unadsorbed protein.

Column measurements have shown that at very low ionic strengths (< 0.1 mM) salts are excluded from Q-Sepharose FF. At slightly higher ionic strengths the exclusion is not as strong as would be predicted when the ion exchanger is considered as an electrically uniform phase. Electrical exclusion only plays a role in a region close to the fibers. At very low ionic strength, however, this region will include the whole pore, and the ion exchanger will behave as an electrically uniform phase.

For proteins electrical exclusion can play a role at higher ionic strengths because proteins are larger and have higher charges than salt ions. Under weak binding conditions pore diffusion is unimportant and our experiments cannot be used to draw conclusions concerning electrical exclusion. With strong binding conditions pore diffusion is important, but, as can be seen in Figure 7, there is a great deal of uncertainty in the pore-diffusion coefficient, so we cannot draw any conclu-

sions here either. However, because of the pore-diffusion coefficient's low value, we believe that electrical exclusion is important. This is discussed in the next subsection.

Pore-diffusion coefficient

In the TPD model the pore-diffusion coefficient was fitted by assuming that it has the same value in each experiment and then calculating the correlation coefficient R^2 for the relation between the binding strength and the surface diffusion coefficient (as in Figure 6). The result is given in Figure 7; the optimum lies at 9×10^{-13} m^2/s, although this value is very uncertain. Another way of estimating it is with a shrinking-core (SC) model, a model in which irreversible adsorption is assumed and in which diffusion to the center of the particle occurs only by unadsorbed proteins. For very strong binding the TPD model should give the same result as the SC model. At the strongest binding the diffusion coefficient found with the SC model is 6×10^{-13} m^2/s. In order to compare it with the pore-diffusion coefficient from the TPD model, it has to be divided by the pore holdup (0.52). The two values are quite close. The pore-diffusion coefficients found with the SC model depend on the binding strength, which suggests that the pore-diffusion coefficient will depend on some parameter related to the binding strength (such as the ionic strength). The fitted pore-diffusion coefficient is not a pure diffusion coefficient, because the partition coefficient (the protein concentration in the pore bulk divided by that in the bulk liquid) also affects the diffusive flux. In our model we assumed a constant partition coefficient equal to the pore holdup ϵ_p. However, the partition constant may vary due to steric and electric exclusion. The fitted pore-diffusion coefficients are therefore the product of a real diffusion coefficient and a partition coefficient.

Comparing the fitted pore-diffusion coefficient with the diffusion coefficient of BSA in liquid (5.9×10^{-11} m^2/s) yields a retardation factor of 50. BSA diffusion coefficients in 6% Sepharose, a nonbinding matrix, have been measured by a chromatographic method by Boyer and Hsu (1992), who found a retardation factor of only 6. Moussaoui et al. (1992) and Johnson et al. (1995) measured them with the fluorescence recovery after photobleaching (FRAP) method, and they found retardation factors of 2.5 and 2.1, respectively. Under nonbinding conditions we measured a retardation factor of 6 (Bosma and Wesselingh, 2000). Apparently pore diffusion (or partitioning) is greatly hindered by adsorbed protein.

During desorption the retardation factor is about 3. This is somewhat high compared to data from the literature. One reason for this difference may be that when desorption occurs the protein concentration in the pores becomes so high that the activity coefficient becomes larger than one.

We investigated whether slow pore diffusion could be ascribed to steric effects due to adsorbed protein. In the TPD model we made the pore-diffusion coefficient dependent on the adsorbed concentration by using various functions to vary the retardation factor between 50 at full adsorption and 3 at full desorption. The correlations between binding strength and surface-diffusion coefficient became much worse. Therefore the hindrance of diffusion is not purely steric. We think that both steric and electric factors affect the hindrance of pore diffusion. Their magnitude will depend on the circumstances.

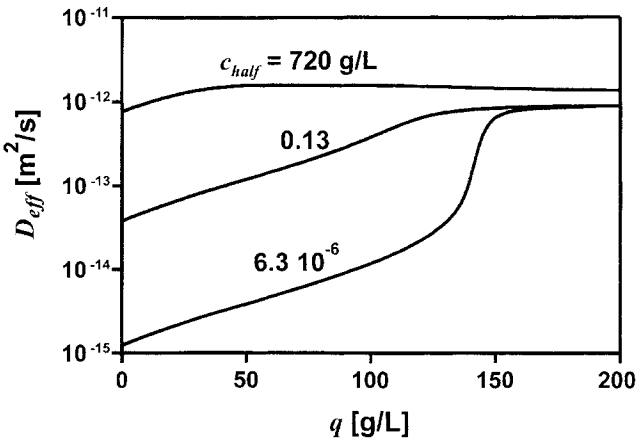

Figure 13. Effective-diffusion coefficient in the particle as a function of the total protein concentration for three half-concentrations.

Yoshida et al. (1994) investigated the diffusion of BSA in chitosan ion exchangers. They found a pore-diffusion coefficient of 2.7×10^{-11} m^2/s with the SC model and 1.0×10^{-11} m^2/s with a parallel diffusion model. The pore-diffusion coefficient in chitosan is higher than that in agarose, as chitosan apparently has larger pores.

The effective-diffusion coefficient

Figure 13 shows the effective-diffusion coefficient vs. the total protein concentration (according to Eq. 8) for three binding strengths. Two limits can be distinguished:

- If there is no binding, the effective-diffusion coefficient will be equal to the pore-diffusion coefficient.
- If the binding is irreversible, the effective-diffusion coefficient will be zero if the surface is not saturated (the surface-diffusion coefficient will be zero) and equal to the pore-diffusion coefficient if the surface is saturated.

The examples in Figure 13 all lie between these two limits. One interesting aspect of the effective-diffusion coefficient for weak binding is that it can become larger than either the surface-diffusion coefficient or the pore-diffusion coefficient. This aspect is caused by the fact that the chemical potential is the real driving force for diffusion.

Relative importance of the diffusion mechanisms

Figure 14 shows that the relative importance of the diffusion mechanisms depends on the binding strength and the concentration. Surface diffusion will always be more important for low concentrations. However, in an experiment there are usually regions of high and of low concentration, so the actual relative importance of the mechanisms cannot be seen in Figure 14.

The fact that we found quite accurate values for the surface-diffusion coefficient but a very uncertain value for the pore diffusion coefficient indicates that surface diffusion is more important. Figure 7 also shows that if we choose the

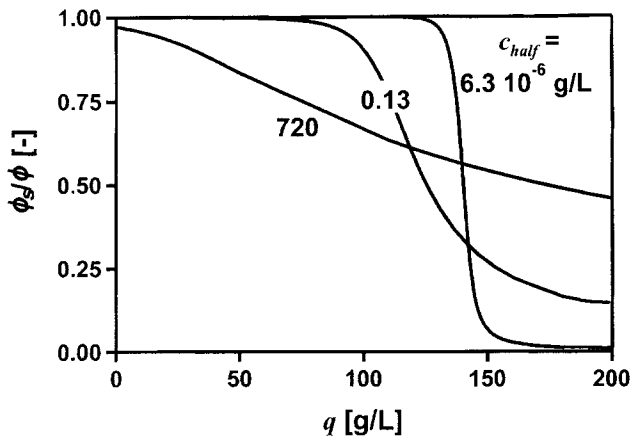

Figure 14. Relative importance of surface diffusion as a function of the total protein concentration for three half-concentrations.

pore-diffusion coefficient an order of magnitude lower, the correlation barely deteriorates. Figure 15 shows the surface-diffusion flux divided by the total diffusion flux when equilibrium is almost reached. Before drawing conclusions from this figure, it must be realized that the concentration is lower during the adsorption, so a larger part of the proteins will be adsorbed and surface diffusion will be more important. It can be seen that pore-diffusion is more important for very strong binding, while surface diffusion is dominant for intermediate and weak binding.

Differences between TPD model and measurements

In three cases we found differences between the results of the TPD model calculations and the experiments:

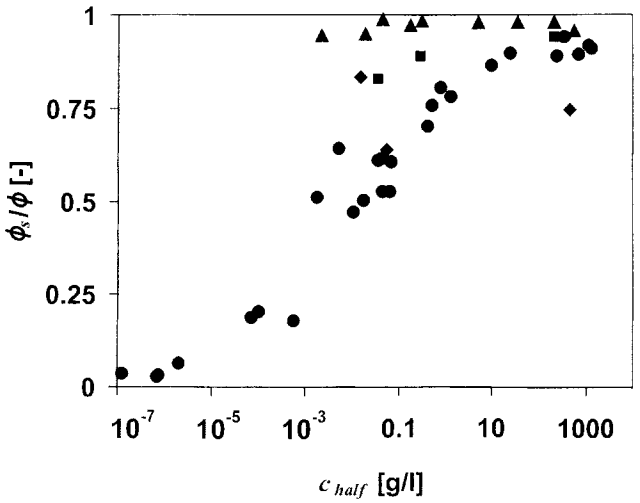

Figure 15. Importance of surface diffusion vs. total diffusion when the equilibrium is almost attained.

Symbols: approximate average protein concentration: △ -2 g/L, □ -5 g/L, ○ -10 g/L, ◇ -15 or 20 g/L.

- It can be seen in Figure 5 that the final attainment of equilibrium takes longer than predicted.
- It can be seen in Figures 8 and 9 that during the adsorption–desorption experiments the measured maximums in the bulk concentration are much larger than the predicted ones.
- It can be seen in Figures 10 through 12 that the measured concentration profiles inside the particle are shallower than the predicted ones.

The second phenomenon can also be seen in the results of Karst Lewus and Carta (1999), who measured the competitive adsorption of two proteins.

All differences can be explained by inhomogeneities in the particle. We think that there are faster than average diffusion paths and slower than average diffusion paths. The fastest route from the surface of the particle to a certain location inside the particle is not necessarily a straight path. The diffusion paths can be likened to the trunk, the branches, and the needles of a Christmas tree.

The first difference mentioned can also be explained by the effect of large particles. This difference is not observed at low starting concentrations (see Figure 4), because the adsorption at the sites that are easy to reach will drain most of the proteins out of the liquid phase.

Conclusions

In this article we have investigated the kinetics of the adsorption of a protein on an ion exchanger. Our main conclusions are as follows:

- In our experimental system surface diffusion (diffusion of adsorbed protein) is the main diffusion mechanism.
- The driving force for surface diffusion is the chemical-potential gradient and not the concentration gradient.
- The effect of pH and the ionic strength on the surface diffusion can be represented simultaneously by the effect of the binding strength.
- When the binding strength increases, the surface-diffusion coefficient decreases sharply. This dependency can be described by an activated jump mechanism.
- When the binding strength becomes very high, pore diffusion becomes important.
- The pore diffusion flux will decrease when the binding strength increases due to the decrease in the concentration of unadsorbed protein.
- Pore diffusion is severely hindered by a combination of steric and electric effects.
- A two-phase diffusion model takes all these effects into account and is therefore the best model for describing the kinetics of the adsorption.
- The two-phase diffusion model still has some deficiencies, the main one being that it does not take inhomogeneities in the particle into account.

Using our experimental system we found that diffusion decreases when binding strength increases. Karst Lewus and Carta (1999) investigated the competitive adsorption of two proteins. One of these proteins (cytochrome c) binds weakly and diffuses rapidly, while the other (lysozyme) binds strongly and diffuses slowly. This indicates that the inverse relation between binding strength and diffusion coefficient is not only valid for one protein but that it can be used as a rule of

thumb when different proteins are compared. Although there are also other factors that are important, such as size, the binding strength is probably the most important one.

Acknowledgments

We thank the Dutch Ministry of Economic Affairs for financial support.

Notation

a = interfacial area, m^{-1}
c = concentration in the bulk, g/L
c_{half} = half-concentration, g/L
c_p = concentration in the pore, g/L
c_{UV} = protein concentration measured by the UV meter, g/L
d_p = particle diameter, m
D_{eff} = effective-diffusion coefficient, m^2/s
D_p = pore-diffusion coefficient, m^2/s
D_s = surface-diffusion coefficient, m^2/s
M = molar mass, kg/mol
q = total concentration in the particle, g/L particle
$\bar{q}$ = small anion concentration in the bulk, M
q_s = adsorbed concentration, g/L particle
r = radius, m
R^2 = correlation defined by

$$R^2 = \frac{[n\Sigma(xy) - (\Sigma x)(\Sigma y)]^2}{[n\Sigma(x^2) - (\Sigma x)^2] \cdot [n\Sigma(y^2) - (\Sigma y)^2]}$$

where n is the number of measured pairs x,y
R_p = particle radius, m
t = time, s
T = temperature, K

Greek letters

δ_l = liquid-side film thickness, m
$\Delta\mu_{ads}$ = free energy of adsorption, J/mol
ϵ = volume fraction
ϵ_p = pore holdup
ϕ = total diffusive flux, m/s·g/L
ϕ_p = diffusive flux in the pore, m/s·g/L
ϕ_s = diffusive flux at the surface, m/s·g/L

Literature Cited

Bosma, J. C., and J. A. Wesselingh, "pH Dependence of Ion Exchange Equilibrium of Proteins," *AIChE J.*, **44**, 2399 (1998).
Bosma, J. C., and J. A. Wesselingh, "Partitioning and Diffusion of Large Molecules in Fibrous Structures," *J. Chromatog.*, **B 743**, 169 (2000).
Boyer, P. M., and J. T. Hsu, "Experimental Studies of Restricted Protein Diffusion in an Agarose Matrix," *AIChE J.*, **38**, 259 (1992).
Calderbank, P. H., and M. B. Moo-Young, "The Continuous Phase Heat and Mass-Transfer Properties of Dispersions," *Chem. Eng. Sci.*, **16**, 39 (1961).
Habbaba, M. M., and K. Ö. "Ülgen, "Analysis of Protein Adsorption to Ion Exchangers in a Finite Bath," *J. Chem. Technol. Biotechnol.*, **69**, 405 (1997).
Johnson, E. M., D. A. Berk, R. K. Jain, and W. M. Deen, "Diffusion and Partitioning of Proteins in Charged Agarose Gels," *Biophys. J.*, **68**, 1561 (1995).
Kapteijn, F., W. J. W. Bakker, G. Zheng, J. Poppe, and J. A. Moulijn, "Permeation and Separation of Light Hydrocarbons through Silicalite-1 Membrane: Application of the Generalized Maxwell-Stefan Equations," *Chem. Eng. J.*, **57**, 145 (1995).
Karst Lewus, R., and G. Carta, "Binary Protein Adsorption on Gel-Composite Ion-Exchange Media," *AIChE J.*, **45**, 512 (1999).
Moussaoui, M., M. Benlyas, and P. Wahl, "Diffusion of Proteins in Sepharose Cl-B Gels," *J. Chromatog.*, **591**, 115 (1992).
Wesselingh, J. A., and R. Krishna, *Mass Transfer in Multicomponent Mixtures*, Delft Univ. Press, Delft, Netherlands (2000).
Yoshida, H., M. Yoshikawa, and T. Kataoka, "Parallel Transport of BSA by Surface and Pore Diffusion in Strongly Basic Chitosan," *AIChE J.*, **40**, 2034 (1994).

Manuscript received Feb. 24, 2000, and revision received Oct. 4, 2000.